# A numerical study on the influence of non-axisymmetric flow perturbations on the hole-tone feedback cycle(Mathematical Aspects and Applications of Wave Phenomena)

AUTHOR(S):

LANGTHJEM, MIKAEL A.; NAKANO, MASAMI

数理解析研究所講究録
第1543巻 2007年 21-30



# A numerical study on the influence of non-axisymmetric flow perturbations on the hole-tone feedback cycle

MIKAEL A. LANGTHJEM, MASAMI NAKANO

Department of Mechanical Systems Engineering,
Faculty of Engineering, Yamagata University,
Jonan 4-chome, Yonezawa-shi, 992-8510 Japan

**Abstract**

The paper is concerned with the hole-tone feedback cycle problem, also known as Rayleigh's bird-call. A methodology for analyzing the influence of non-axisymmetric perturbations of the jet on the sound generation is described. In future experiments, these perturbations will be applied at the jet nozzle via piezoelectric or electro-mechanical actuators, placed circumferentially inside the nozzle at its exit. The mathematical model, which is the subject of the present paper, is based on a three-dimensional vortex method. The nozzle and the holed end-plate are represented by quadrilateral vortex panels, while the shear layer of the jet is represented by vortex rings, composed of vortex filaments. The sound generation is described mathematically using the Powell-Howe theory of vortex sound. The aim of the work is to understand the effects of a variety of flow perturbations, in order to control the flow and the accompanying sound generation.

Keywords: aeroacoustics, self-sustained flow oscillations, three-dimensional vortex method

## 1 Introduction

Self-sustained fluid oscillations can occur in a variety of practical applications where a shear layer impinges upon a solid structure [1]. The oscillations are the cause of sound generation, which typically is powerful. In cases of music instruments (flutes, etc.) and whistles, sound generation is, of course, the aim. By engineering applications however, the sound generation is, in most cases, an unwanted, annoying side effect.

The present paper is concerned with the so-called hole-tone problem [2, 3]. The common teapot whistle is an example of utilization of the sound generation in this system. The steam jet, issuing from a nozzle, passes through a similar hole in a plate, placed a little downstream from the nozzle. The shear layer of the jet is unstable and rolls up into a large, coherent vortex ('smoke-ring'). This large vortex cannot pass through the hole in the plate and hits the edge of the hole, where it creates a pressure disturbance. The disturbance is thrown back (with the speed of sound) to the nozzle, where it disturbs the shear layer. This initiates the roll-up of a new coherent vortex. In this way an acoustic feedback loop is formed. Figure 1(a) illustrates the principle of the hole-tone phenomenon. Figure 1(b) shows an experimental realization, with the vortex roll-up visualized by the smoke wire technique [4].

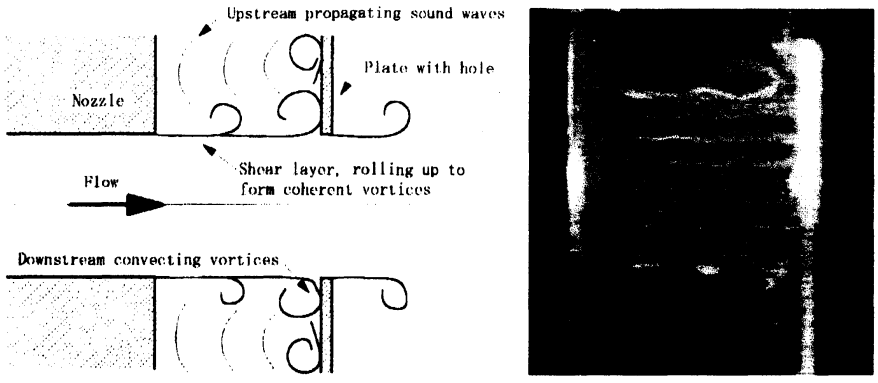


(a) (b)

Figure 1: (a) Geometry and physical features of the hole-tone problem. (b) Flow visualization of the vortex roll-up [4].

The basic dynamics of the hole-tone feedback system was studied numerically in Ref. [5], using an axisymmetric vortex element method, combined with an aeroacoustic model based on Curle's equation [6]. It was found that this methodology could predict the fundamental characteristics of the problem quite well, in particular the fluid-dynamic characteristics.

The bird-call, as described in Rayleigh's *The Theory of Sound* [2] is a small whistle for simulating birdsong. It has been speculated at some point that the hole-tone phenomenon may be the fundamental mechanism of real whistled birdsong, although the idea seems to be abandoned at present [7]. The hole-tone system is however a part of many engineering systems, where sound generation is unwanted. Examples include automobile intake- and exhaust systems, gas/steam distribution systems (bellows, valves, etc.), and solid-propellant rocket motors. In these cases, if a geometry which avoids the sound-generation cannot easily be obtained, a control method which can eliminate, or at least suppress, the sound generation is desirable.

Nakano *et al.* [4] studied experimentally a forced excitation strategy to eliminate the hole-tone feedback cycle in the system depicted in Fig. 1. The shear layer near the nozzle exit was excited acoustically by means of an excitation chamber equipped with six loudspeakers, placed equidistantly around the circumference. By harmonic, axisymmetric excitation at frequencies away from the fundamental frequency $f_0$, noise level reductions (at $f_0$) of up to 6 dB were achieved. A part of these experiments were simulated numerically in Ref. [8]. It was found that forced acoustic excitation of the shear layer could suppress the sound pressure level, but to a lesser degree than in the experiments.

The aim of the present work is to develop a simple and efficient numerical method for a full three-dimensional simulation of the hole-tone problem with the jet subjected to *non-axisymmetric* 'mechanical' ('non-acoustic') perturbations, by piezoelectric or electro-mechanical actuators mounted around the circumference at the nozzle exit, similar to the experimental concept of Kasagi [9]. With this concept, a variety of excitation modes and control laws can be realized. Kasagi [9] presents some very interesting experimental results related to a free jet. A purpose of the present work is to investigate how, and to what extent, various excitation modes (with various degrees of symmetry) are able to suppress the noise generation in the hole-tone problem.

Similar to our previous study [5], the present one is also based on a vortex method. Vortex methods are particularly well-suited for problems like the present, where vorticity is confined

to shear layers constituting only a small part of the overall fluid volume [10]. It has recently been shown [11] that numerical simulations with three-dimensional vortex filaments produce characteristics of turbulent flows which agree well with experiments and direct numerical simulations (based on the Navier-Stokes equations). The present work is based on the *vortex filament method*, similar to the work of Cortelezzi and Karagoizian [12], dealing with a jet in crossflow. Alternatively, the *vortex particle method* could have been chosen; this is done, for example, in the work of Kiya *et al.* [13], dealing with forced excitation of a free jet.

The paper also includes a discussion of the acoustic modelling, although no numerical results are presented. This includes an acoustic feedback model, e.g. a model of the back-reaction from the acoustic field onto the free vortices. The sound pressure is computed using the vortex sound model of Powell [14] and Howe [15]. As in Lighthill's original acoustic analogy [16], it is assumed in the vortex sound theory that there is no acoustic back-reaction from the acoustic field to the sound-generating background flow. Yet it is thought to be plausible to include an acoustic feedback model in connection with a time-stepping simulation approach, as the present.

## 2 Flow model

### (a) *Modelling of the jet*

The shear layer of the jet issuing from the nozzle is represented in a lumped form, by a 'necklace' of discrete vortex rings. These rings are disturbed mechanically at the nozzle exit such that they loose their natural axisymmetric form, and are thus represented by three-dimensional vortex filaments. The induced velocity $\mathbf{u}_i = (u_1, u_2, u_3)_i$, at position $\mathbf{x}_i = (x_1, x_2, x_3)_i$ and time $t$, from $J$ vortex rings represented by the space curves $\mathbf{r}_j(\xi, t)$, $j = 1, 2, \ldots, J$, is given by [17]

$$\mathbf{u}_i(\mathbf{x}_i, t) = -\sum_{j=1}^{J} \frac{\Gamma_j}{4\pi} \int_{\xi} \frac{[\mathbf{x}_i(t) - \mathbf{r}_j(\xi, t)] \times \partial \mathbf{r}_j / \partial \xi}{(|\mathbf{x}_i(t) - \mathbf{r}_j(\xi, t)|^2 + \alpha \sigma_j^2(\xi, t))^{\frac{3}{2}}} d\xi, \tag{1}$$

where $\Gamma_j$ is the strength (circulation) of the $j$'th vortex, $\xi$ is a material (vortex) coordinate, and $\sigma_j(\xi, t)$ is the core radius. $\alpha$ represents the vorticity distribution within the core. An analytical expression for this parameter can be derived [17]. For a Gaussian distribution, $\alpha \approx 0.413$.

The space curves $\mathbf{r}_j(\xi, t)$ are discretized by employing $K$ marker points on each curve (vortex ring), connected via cubic splines. These splines are expressed in the form of Ferguson curve segments (which in turn are based on Hermite interpolation). The integration is carried out using Gauss-Legendre quadrature. [A simple linear interpolation was however employed to produce the numerical examples in Section 4 of the present paper.]

A vortex ring is released from the nozzle at each time step in the simulation. [Earlier studies [5] have shown that the vortex shedding from the hole in the end plate is insignificant.] The strength of the vortex ring to be released is dictated by the Kutta condition, which demands that the pressure a little above the nozzle edge equals the pressure a little below.

The convection velocity of a shed vortex ring is dictated by the induced velocities from all other vortex rings, plus the self-induced velocity, as indicated by (1). The positions $\mathbf{r}_i$ of the shed vortex filament ring marker points are updated by solving numerically the system of ordinary differential equations

$$\frac{\mathrm{d}\mathbf{r}_i(t)}{\mathrm{d}t} = \mathbf{u}_i(\mathbf{r}_i, t), \qquad i = 1, 2, \ldots, J \times K. \tag{2}$$

Except for the viscous effect simulated by the Kutta condition, the computations are basically inviscid. This means that the vortex rings keep their strengths throughout the simulation, once

released. The volume of each individual ring must thus be kept constant; this constraint is imposed via the equations

$$\frac{d}{dt}(\sigma_j^2 \ell_j) = 0, \quad j = 1, 2, \ldots, J \times K, \tag{3}$$

where $\ell_j$ is the instantaneous length of the $j$'th filament. There is however one exception to this 'principle'. During interaction with other vortex rings, stretching and folding into 'hairpins' may occur. When the fold angle is beyond a certain threshold value, a hairpins is removed and the the 'loose ends' reconnected, in accordance with the idea proposed by Chorin [18]. Thereby the volume of the vortex ring is reduced. This implies a reduction in the energy of the ring, and amounts to a simple dissipation mechanism.

(*b*) *Modelling of the solid surfaces*

The solid surfaces are represented by quadrilateral vortex panels, made up of four straight vortex filaments, as indicated by Fig. 2. The inviscid boundary condition of zero normal velocity is imposed at control points in the center of these panels. The mean jet flow is provided by a number of panels placed on the 'back' of the nozzle tube. The strengths of the bound vortex panels are dictated by the boundary conditions and by the mean jet velocity.

The mechanical/piezoelectric actuator system is simulated by periodical deformations of the nozzle end section, as illustrated by Fig. 3.

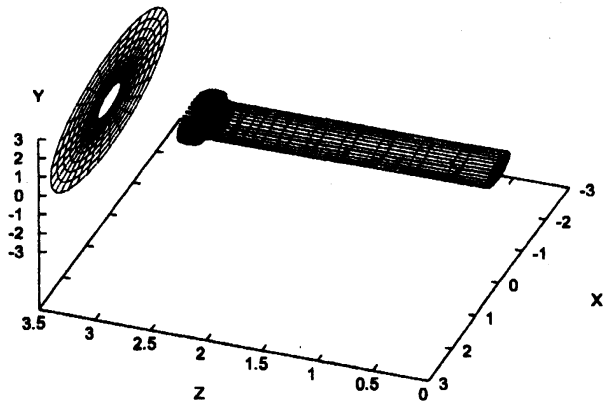


Figure 2: Distribution of bound vortex filament panels on the nozzle and the end plate. The startup vortex of the free jet is also shown in the figure. [In the text the notation $\mathbf{x} = (x_1, x_2, x_3)$ is used, rather than the notation $(x, y, z)$ shown in this and in the following figures.]

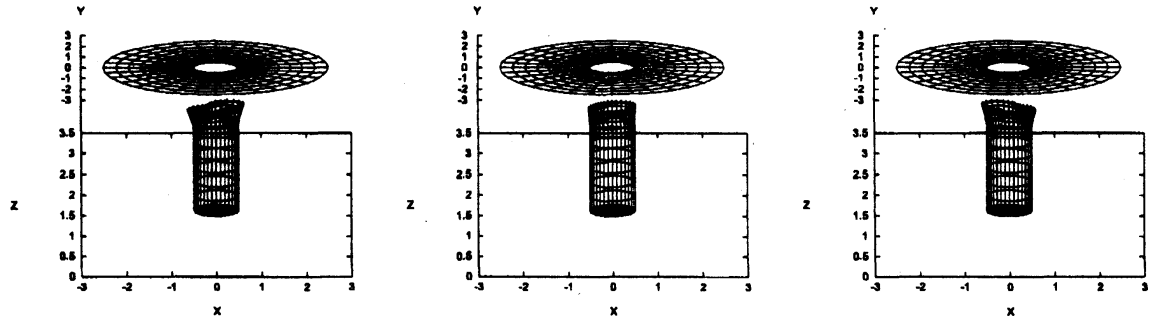

Figure 3: Illustration of the perturbation mechanism (actuator model). [For purpose of illustration the amplitude is exaggerated.]

## 3 Aeroacoustic model

*(a) The vortex sound approach of Powell and Howe*

The concept of vortex sound, introduced by Powell [14] and developed further by Howe [15], is probably the most efficient formulation in connection with a vortex element method [19]. In Howe's formulation the sound emission is, for low Mach-number flows, described by the inhomogeneous wave equation

$$\frac{1}{c_0^2}\frac{\partial^2 B}{\partial t^2} - \nabla^2 B = \nabla \cdot \mathbf{L}, \tag{4}$$

where $B(\mathbf{x},t)$ is the stagnation enthalpy, and $\mathbf{L} = \boldsymbol{\omega} \times \mathbf{u}$ is the vortex force, with the vorticity $\boldsymbol{\omega}$ given by $\nabla \times \mathbf{u}$. The relation between the enthalpy $B$ and the acoustic pressure $p$ can be expressed as [20]

$$\frac{\partial p}{\partial t} = \rho_0 \left( \frac{\partial B}{\partial t} + \mathbf{u} \cdot \nabla B \right) = \rho_0 \frac{DB}{Dt}. \tag{5}$$

In the far field, the convective term disappears, giving the simple relation $p(\mathbf{x},t) \approx \rho_0 B(\mathbf{x},t)$.

The solution to (4) is given by

$$B(\mathbf{x},t) = -\int_\tau \int_{\mathbf{y}} \nabla_y G(\mathbf{x},\mathbf{y},t-\tau) \cdot \mathbf{L} d\mathbf{y} d\tau. \tag{6}$$

Here $G(\mathbf{x},\mathbf{y},t-\tau)$ is a Green's function which satisfies the boundary value problem

$$\frac{1}{c_0^2}\frac{\partial^2 G}{\partial \tau^2} - \nabla_y^2 G = \delta(\mathbf{x}-\mathbf{y})\delta(t-\tau), \tag{7}$$

$$G = 0 \text{ for } t < \tau, \text{ and } \frac{\partial G}{\partial \mathbf{n}} = 0 \text{ on } S.$$

$S$ symbolizes the surface of the end plate, and $\mathbf{n} = (n_1, n_2, n_3)$ its normal vector. Furthermore, $\mathbf{x}$ is an observation point and $\mathbf{y}$ a source point (i.e., a point on a vortex ring). An approximate solution to (7), correct to dipole order when $S$ is acoustically compact, is given by the so-called compact Green's function [19, 20]

$$G(x,y,t-\tau) \approx \frac{\delta\left(t-\tau-|\mathbf{X}-\mathbf{Y}|/c_0\right)}{4\pi|\mathbf{X}-\mathbf{Y}|}, \tag{8}$$

where $\mathbf{X} = (X_1(\mathbf{x}), X_2(\mathbf{x}), X_3(\mathbf{x}))$, with $X_i = x_i - \varphi_i^*(\mathbf{x})$, and similarly for $\mathbf{Y}$. The function $\varphi_i^*(\mathbf{x})$ is the velocity potential of the flow produced by moving the surface $S$ (the end plate) at unit speed in the $i$-direction. In the present problem, only $\varphi_3^*$ will be non-zero if it is assumed that the thickness of the end plate is vanishingly small. On $S$, it satisfies the relation $\partial\varphi_3^*/\partial x_3 = n_3$. Based on the employed vortex panel representation of the solid surfaces, $\varphi_3^*$ is easily determined numerically.

The final expression for the stagnation enthalpy $B$ takes the form

$$\begin{aligned} B(\mathbf{x},t) = &- \sum_{j=1}^{3} \frac{1}{4\pi} \int_{\mathbf{y}} \left[ (\boldsymbol{\omega} \times \mathbf{u})_j(\mathbf{y},t_r) \frac{X_j - Y_j}{|\mathbf{X}-\mathbf{Y}|^3} \nabla Y_j d^3\mathbf{y} \right]_{t_r} \\ &- \sum_{j=1}^{3} \frac{1}{4\pi c_0} \int_{\mathbf{y}} \left[ \frac{\partial}{\partial t} \left\{ (\boldsymbol{\omega} \times \mathbf{u})_j(\mathbf{y},t_r) \frac{X_j - Y_j}{|\mathbf{X}-\mathbf{Y}|^2} \nabla Y_j \right\} d^3\mathbf{y} \right]_{t_r}. \end{aligned} \tag{9}$$

The square brackets with subscript $t_r$ indicate evaluation at the retarded time $t_r = t - |\mathbf{x}-\mathbf{y}|/c_0$. In the numerical implementation, the integrals over 'source space' $\mathbf{y}$ is replaced by summation

over all free vortex filament rings. The number of free vortices typically becomes very large. For numerical efficiency, it is thus important that this summation is carried out simultaneously with that in (2).

The first term in (9) will dominate in the near field; the second term in the far field. In most aeroacoustic analyses the interest is only in the far field sound, and the first term is discarded. The reason for keeping it here is that the far field sound pressure is difficult to measure in the experiments [4], due to reflections from the surroundings. [An anechoic chamber is not available at present.] Hence only the near field pressure is measured, and has to be computed as well. Another reason for keeping the near field term is that (9) is used also to evaluate the acoustic feedback. This is the subject of the following section.

(*b*) *Acoustic feedback model*

For low Mach number flows it is known that the feedback mechanism works hydrodynamically (i.e., instantaneously, without acoustic/compressibility effects), as the nozzle then lies only a fraction of the fundamental acoustic wavelength away from the end plate. In our earlier work [5], based on Curle's equation, it was found however, that an acoustic feedback signal ('compressibility correction') reinforced the characteristic hole-tone frequency component and its higher harmonics. It is thus found interesting to investigate the effect of acoustic feedback also in the present vortex sound model, although it is understood that near field acoustic variables are difficult to compute.

The acoustically induced flow, with velocity $\mathbf{v}(\mathbf{x},t)$, is assumed to be a potential flow, superimposed on the vortical 'background flow' (with velocity $\mathbf{u}(\mathbf{x},t)$). The acoustic pressure $p(\mathbf{x},t)$ and the acoustic (disturbance) velocity $\mathbf{v}(\mathbf{x},t)$ is then related via the expression

$$\frac{\partial p}{\partial t} = -\nabla \cdot \mathbf{v}, \tag{10}$$

or via a potential function, $\Psi(\mathbf{x},t)$, as

$$p = \rho_0 \frac{\partial \Psi}{\partial t}, \quad \mathbf{v} = -\nabla \Psi. \tag{11}$$

Equations (5) and (11) give the relation

$$\mathbf{v} = \underbrace{-\int \nabla B dt}_{\mathbf{v}^*} \underbrace{-\int\int \nabla(\mathbf{u}\cdot\nabla B) d\bar{t} dt}_{\mathbf{v}_{\mathrm{conv}}}. \tag{12}$$

Only the first (non-convective) term $\mathbf{v}^*(x,t)$ of (12) will be shown here. Using (9), it is given by

$$\begin{aligned} v_k^*(\mathbf{x},t) &= -\sum_{j=1}^{3} \frac{1}{4\pi c_0^2} \int_{\mathbf{y}} \left[ \frac{\partial}{\partial t} \left\{ (\boldsymbol{\omega}\times\mathbf{u})_j \frac{X_j - Y_j}{|\mathbf{X}-\mathbf{Y}|^3} \nabla Y_j \nabla X_k (X_k - Y_k) \right\} d^3\mathbf{y} \right]_{t_r} \\ &+ \sum_{j=1}^{3} \frac{1}{4\pi c_0} \int_{\mathbf{y}} \left[ (\boldsymbol{\omega}\times\mathbf{u})_j \frac{X_j - Y_j}{|\mathbf{X}-\mathbf{Y}|^4} \nabla Y_j \nabla X_k (X_k - Y_k) d^3\mathbf{y} \right]_{t_r} \\ &- \sum_{j=1}^{3} \frac{1}{4\pi} \int_{-\infty}^{t} \int_{\mathbf{y}} \left[ (\boldsymbol{\omega}\times\mathbf{u})_j \frac{3(X_j - Y_j)}{|\mathbf{X}-\mathbf{Y}|^5} \nabla Y_j X_k (X_k - Y_k) d^3\mathbf{y} \right]_{t_r} d\tau \\ &- \sum_{j=1}^{3} \frac{1}{4\pi c_0} \int_{\mathbf{y}} \left[ (\boldsymbol{\omega}\times\mathbf{u})_j \frac{\nabla X_k \nabla Y_k}{|\mathbf{X}-\mathbf{Y}|^2} d^3\mathbf{y} \right]_{t_r} + \sum_{j=1}^{3} \frac{1}{4\pi} \int_{-\infty}^{t} \int_{\mathbf{y}} \left[ (\boldsymbol{\omega}\times\mathbf{u})_j \frac{\nabla X_k \nabla Y_k}{|\mathbf{X}-\mathbf{Y}|^3} d^3\mathbf{y} \right]_{t_r} d\tau. \end{aligned} \tag{13}$$

These acoustic velocities act as disturbances to the hydrodynamic velocity field, and are imposed onto the vortices located near the nozzle exit.

## 4 Numerical examples

(*a*) *Start-up jet*

The calculations of the present paper were carried out for a setup with nozzle and end plate hole diameter $d_0$ equal to 50 mm. The outer diameter of the end plate is 250 mm. The gap length $L$ is 50 mm, e.g., equal to $d_0$. The mean velocity $u_0$ of the air-jet is 10 m/s. At 20 °C this corresponds to a Reynolds number $Re = u_0 d_0/\nu \approx 3.3 \times 10^4$ and a Mach number $M = u_0/c_0 \approx 0.03$, where the speed of sound $c_0 = 340$ m/s and the kinematic viscosity $\nu = 1.5 \times 10^{-5}$ m$^2$/s.

The vortex rings are discretized into 24 control points in azimuthal direction ($K = 24$). Linear interpolation between the control points is used to produce the examples to follow; the integrals (1) can then be evaluated analytically. The first order Euler method is employed for the time-integration of (2). The time-step $\Delta t = 0.025 d_0/u_0$.

Figure 4 shows the side view of the impulsively started flow. A 'birds eye-view' of the system, after 500 time-steps, is shown in Fig. 5.

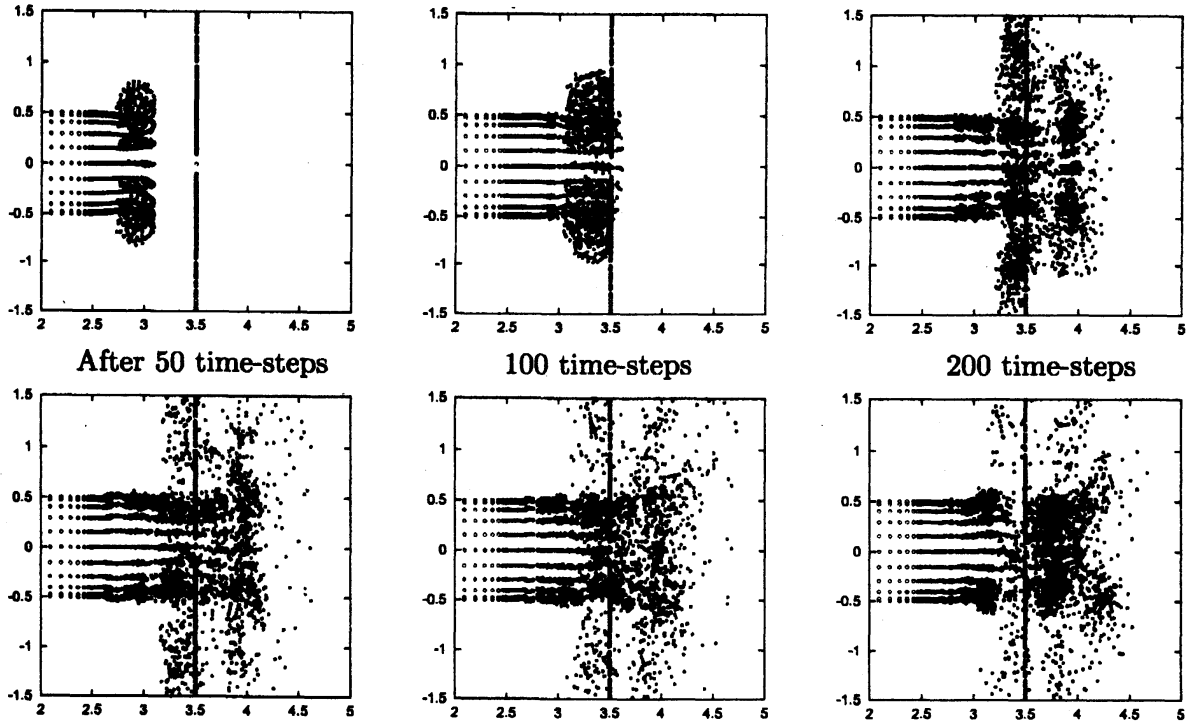


Figure 4: Side view of the jet after impulsive start-up. The nozzle exit is at the abscissa position 2.5; the end plate with hole at position 3.5.

(*b*) *Influence of non-axisymmetric perturbations*

Figure 6 illustrates the influence of the nozzle excitation shown in Fig. 3. The excitation amplitude is $r_0/20$; the frequency is 300 Hz. Part (a) of Fig. 6 shows a sequence of side view 'snapshots' for the non-perturbed jet, while part (b) is for the perturbed jet. The coherent 'smoke ring' which develops in part (a) is clearly destroyed by the perturbations in part (b).

Figure 7 (a) shows the pressure on the end plate, near the edge of the hole. The signal shown is the mean pressure, averaged over all control points at one particular radius, slightly larger than that of the hole. [The large peak at $t \approx 0.035$ s is caused by the impingement of the

start-up vortex onto the end plate.] The corresponding frequency spectrum is shown in part (b). Part (c) shows the pressure signal for the perturbed flow, and part (d) the to (c) corresponding frequency spectrum.

As in part (a) of Fig. 7, part (c) shows the pressure averaged over the circumference. The perturbations imply that negative and positive pressure contributions cancel out. It is then not surprising that the pressure peaks disappear. From a hydrodynamic point of view, the averaged pressure signal is not really interesting. But from an acoustic point of view, the intermediate/far field dipole sound contribution is due to the overall pressure fluctuations on the plate. The result gives thus an indication that non-axisymmetric perturbations may be effective in cancelling the flow-induced hole-tone sound.

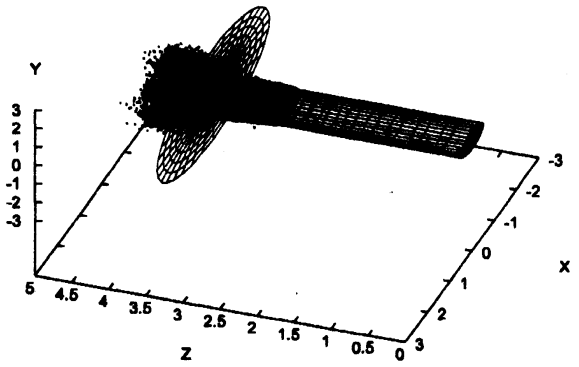


Figure 5: Birds eye-view of the system after 500 time-steps.

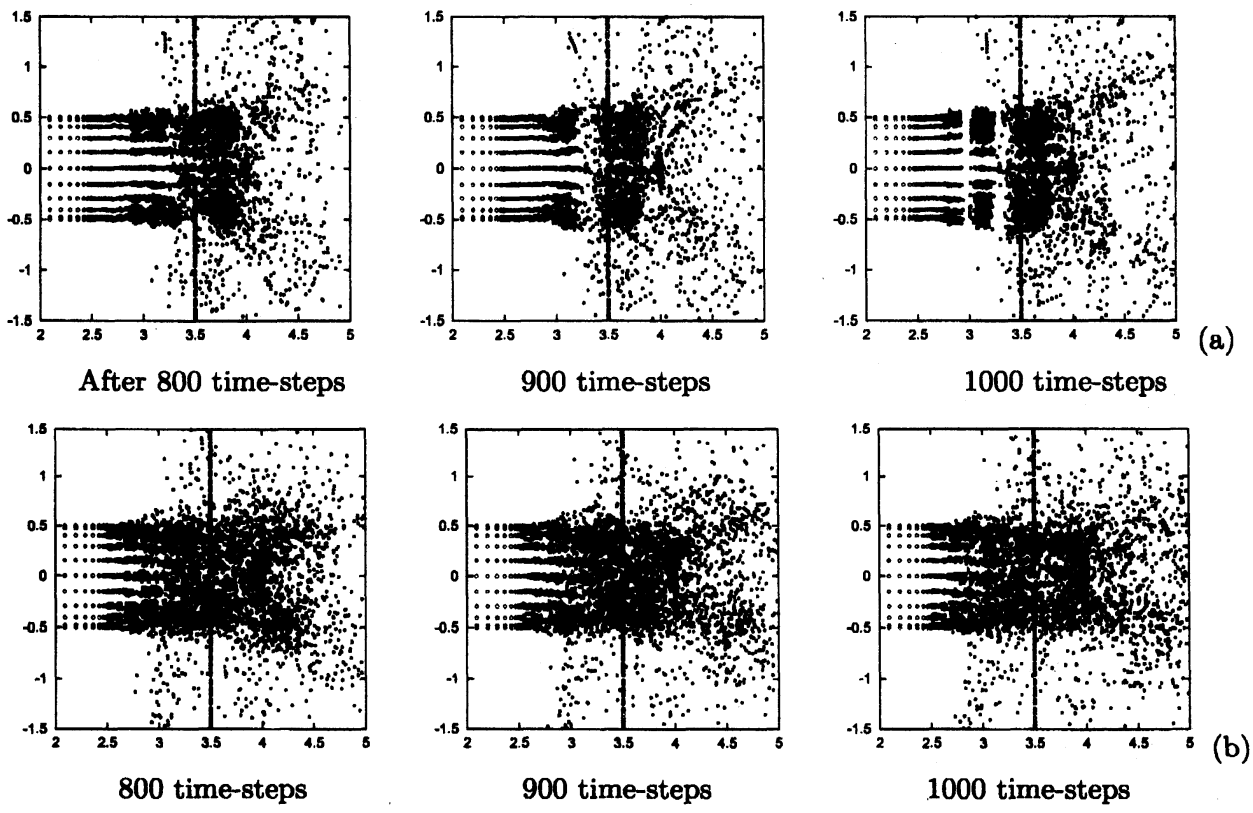


Figure 6: Influence of nozzle perturbations (as shown in Fig. 3) on the appearance of the jet. (a) Unperturbed; (b) perturbed. A side view of the jet is shown. The nozzle exit is at the abscissa position 2.5; the end plate with hole at position 3.5.

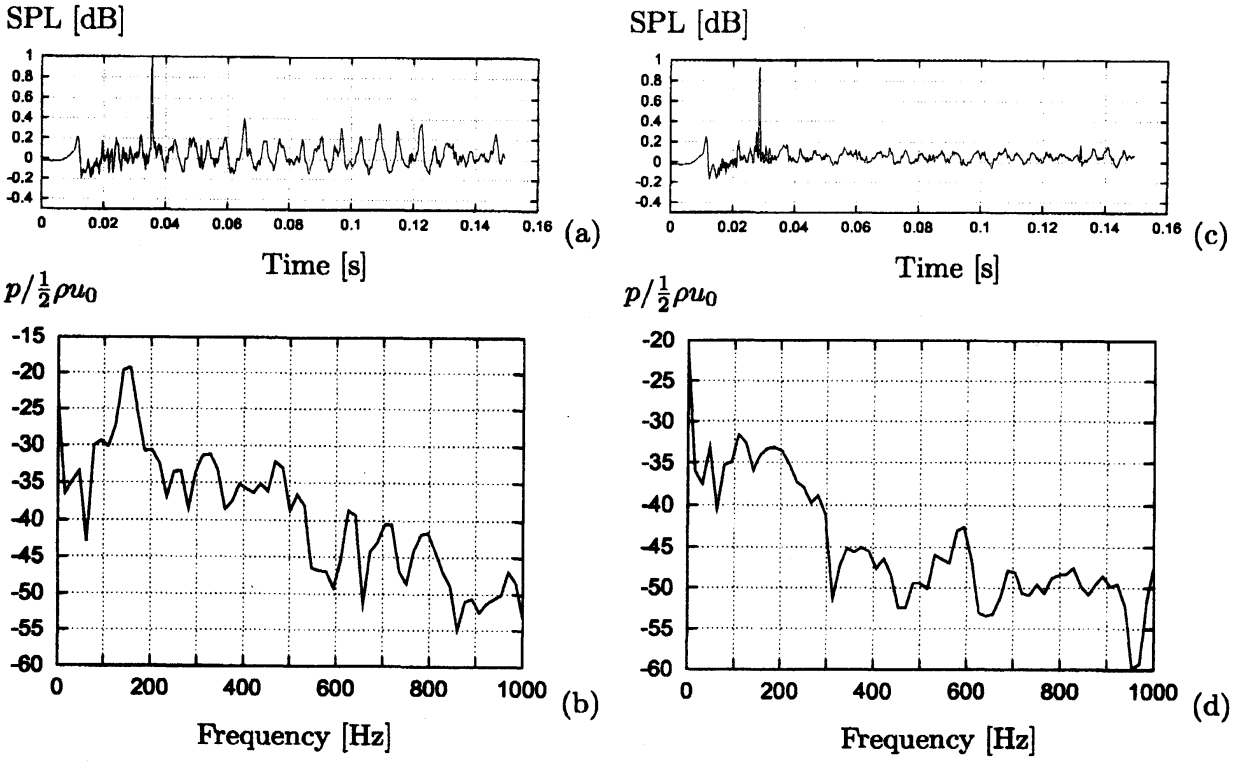


Figure 7: (a) Pressure fluctuations near the hole in the end plate. The signal shown is the average of the pressure at all control points at one particular radius, around the circumference. (b) The to (a) corresponding frequency spectrum. (c) Pressure fluctuations in the case of a perturbed jet (averaged signal, as in(a)). (d) The to (c) corresponding spectrum.

## 5 Summary

In this paper a three-dimensional vortex filament method, combined with an acoustic feedback model based on the theory of vortex sound, has been constructed. The purpose of the work is to study the influence of non-axisymmetric flow perturbations on the flow field and the sound generation in the hole-tone feedback cycle problem. A few preliminary numerical studies have been presented. Comprehensive parameter studies are ongoing.

## 6 Acknowledgement

The support of the present project through a JSPS Grant-in-Aid for Scientific Research (No. 18560152) is gratefully acknowledged.

## References

[1] D. Rockwell, E. Naudascher, "Self-sustained oscillations of impinging free shear layers," Annu. Rev. Fluid Mech. **11**, 67-94 (1979).

[2] Lord Rayleigh, *The Theory of Sound*, Vol. II (Dover, New York, 1896, re-issued 1945).

[3] R.C. Chanaud, A. Powell, "Some experiments concerning the hole and ring tone," J. Acoust. Soc. Am. **37**, 902-911 (1965).

[4] M. Nakano, D. Tsuchidoi, K. Kohiyama, A. Rinoshika, K. Shirono, "Wavelet analysis on behavior of hole-tone self-sustained oscillation of impinging circular air jet subjected to acoustic excitation," (In Japanese) Kashikajouhou **24**, 87-90 (2004).

[5] M. A. Langthjem, M. Nakano, "A numerical simulation of the hole-tone feedback cycle based on an axisymmetric discrete vortex method and Curle's equation," J. Sound and Vibr. **288**, 133-176 (2005).

[6] N. Curle, "The influence of solid boundaries upon aerodynamic sound," Proc. Roy. Soc. Lond. **A** 231, 505-514 (1955).

[7] G. J. L. Beckers, R. A. Suthers, C. t. Cate, "Pure-tone birdsong by resonance filtering of harmonic overtones," Proc. Nat. Acad. Sci. **100**, 7372-7376 (2003).

[8] M. A. Langthjem, M. Nakano, "The jet hole-tone oscillation cycle subjected to acoustic excitation: A numerical study based on an axisymmetric vortex method," in *Jets, Wakes and Separated Flows* (JSME), edited by T. Shakouchi, F. Durst, and K. Toyoda , pp. 745-750, 2005.

[9] N. Kasagi, "Toward smart control of turbulent jet mixing and combustion," in *Jets, Wakes and Separated Flows* (JSME), edited by T. Shakouchi, F. Durst, and K. Toyoda, pp. 45-53, 2005.

[10] G.-H. Cottet, P. D. Koumoutsakos, *Vortex Methods: Theory and Practice*, (Cambridge University Press, Cambridge, 2000).

[11] P. S. Bernard, "Turbulent flow properties of large-scale vortex systems," Proc. Nat. Acad. Sci. **103**, 10174-10179 (2006).

[12] L. Cortelezzi, A. R. Karagozian, "On the formation of the counter-rotating vortex pair in transverse jets," J. Fluid Mech. **446**, 347-373 (2001).

[13] M. Kiya, Y. Ido, H. Akiyama, "Vortical structure in forced unsteady circular jet: Simulation by 3D vortex method," in *Vortex Flows and Related Numerical Methods II* (ESAIM Proc.), edited by Y. Gagnon, G.-H. Cottet, D. G. Dritschel, A. F. Ghoniem, and E. Meiburg, pp. 503-520, 1996.

[14] A. Powell, "Theory of vortex sound," J. Acoust. Soc. Am. **36**, 177-195 (1964).

[15] M. S. Howe, "Contributions to the theory of aerodynamic sound, with applications to excess jet noise and the theory of the flute," J. Fluid Mech. **71**, 625-673 (1975).

[16] M. J. Lighthill, "On sound generated aerodynamically. I. General theory," Proc. Roy. Soc. Lond. **A** 211, 564-587 (1952).

[17] A. Leonard, "Computing three-dimensional incompressible flows with vortex elements," Annu. Rev. Fluid Mech. **17**, 523-559 (1985).

[18] A. J. Chorin, "Hairpin removal in vortex interactions II," J. Comp. Phys. **107**, 1-9 (1993).

[19] M. S. Howe, "Vorticity and the theory of aerodynamic sound," J. Engng. Math. **41**, 367-400 (2001).

[20] M. S. Howe, *Theory of Vortex Sound*, (Cambridge University Press, Cambridge, 2003).